**Fig. 4.** Comparison of the size of the metacommunity species pool, as predicted by the Poisson log-normal distribution (horizontal axis) and the jackknife estimator (vertical axis), with standard errors (24). The diagonal line is the unity line (log-normal estimate = jackknife estimate). Each point corresponds to one habitat type within each metacommunity. The two sets of estimates exhibit excellent fit to the unity line (r^2 = 0.98 and 0.94 for corals and fishes, respectively).
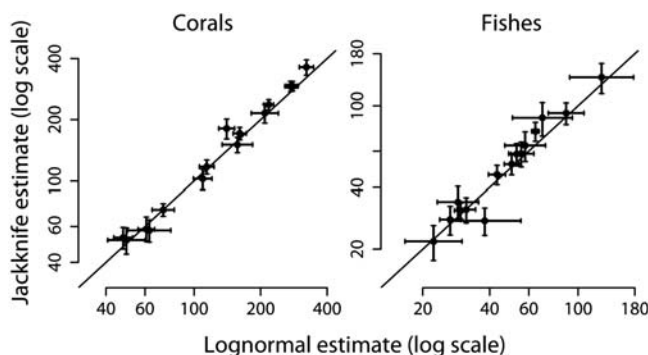
log-normal model agree with predictions from the nonparametric jackknife estimator, which makes no assumptions about the form of the underlying distribution of numerical abundance (Fig. 4).

The search for a limited suite of processes that accounts for consistent patterns in species' relative abundances has occupied ecologists for at least a half century (1); this search has accelerated as the worsening biodiversity crisis has focused attention on the need to understand how high-diversity communities are structured (12, 13). Our results lend strong support to a classical, but controversial, null hypothesis regarding community structure: The shape of species-abundance distributions arises as a general consequence of environmental stochasticity, through its effects on population dynamics. This finding underscores the importance of robust conservation strategies that adequately encompass the spectrum of environmental variability to which coral reef organisms are exposed. Accordingly, conservation efforts should expand in scale and scope, moving beyond localized protected areas and toward a seascape approach (28). Given the accelerating pace of coral reef habitat loss worldwide (21), addressing this challenge remains an urgent priority.

References and Notes

1. R. H. MacArthur, *Proc. Natl. Acad. Sci. U.S.A.* **43**, 293 (1957).
2. M. L. Taper, P. A. Marquet, *Am. Nat.* **147**, 1072 (1996).
3. E. Pachepsky, J. W. Crawford, J. L. Bown, G. Squire, *Nature* **410**, 923 (2001).
4. D. Tilman, *Proc. Natl. Acad. Sci. U.S.A.* **101**, 10854 (2004).
5. J. T. Wootton, *Nature* **433**, 309 (2005).
6. R. A. Fisher, A. S. Corbett, C. B. Williams, *J. Anim. Ecol.* **12**, 42 (1943).
7. F. W. Preston, *Ecology* **43**, 185 (1962).
8. S. Nee, P. H. Harvey, R. M. May, *Proc. R. Soc. London Ser. B* **243**, 161 (1991).
9. A. E. Magurran, P. A. Henderson, *Nature* **422**, 714 (2003).
10. B. J. McGill, *Ecol. Lett.* **6**, 766 (2003).
11. D. Tilman, *Ecology* **75**, 2 (1994).
12. S. W. Hubbell, *The Unified Neutral Theory of Biodiversity and Biogeography* (Princeton Univ. Press, Princeton, NJ, 2001).
13. M. Tokeshi, *Species Coexistence: Ecological and Evolutionary Perspectives* (Blackwell, Oxford, 1999).
14. S. Engen, R. Lande, *J. Theor. Biol.* **178**, 325 (1996).
15. S. Engen, R. Lande, *Math. Biosci.* **132**, 169 (1996).
16. R. V. Sole, D. Alonso, A. McKane, *Philos. Trans. R. Soc. London Ser. B* **357**, 667 (2002).
17. N. Mouquet, M. Loreau, *Am. Nat.* **162**, 544 (2003).
18. R. M. May, in *Ecology and Evolution of Communities*, M. L. Cody, J. M. Diamond, Eds. (Harvard Univ. Press, Cambridge, MA, 1975), pp. 81–120.
19. B. J. McGill, *Nature* **422**, 881 (2003).
20. D. R. Bellwood, T. P. Hughes, *Science* **292**, 1532 (2001).
21. T. P. Hughes *et al.*, *Science* **301**, 929 (2003).
22. D. R. Bellwood, T. P. Hughes, C. Folke, M. Nystrom, *Nature* **429**, 827 (2004).
23. D. R. Bellwood, A. S. Hoey, J. H. Choat, *Ecol. Lett.* **6**, 281 (2003).
24. Materials and methods are available as supporting material on *Science* Online.
25. I. Volkov, J. R. Banavar, S. P. Hubbell, A. Maritan, *Nature* **424**, 1035 (2003).
26. M. Williamson, K. J. Gaston, *J. Anim. Ecol.* **74**, 409 (2005).
27. P. C. Wainwright, D. R. Bellwood, M. W. Westneat, J. R. Grubich, A. S. Hoey, *Biol. J. Linn. Soc.* **82**, 1 (2004).
28. T. P. Hughes, D. R. Bellwood, C. Folke, R. S. Steneck, J. Wilson, *Trends Ecol. Evol.* **20**, 380 (2005).
29. D. R. Bellwood, T. P. Hughes, S. R. Connolly, J. E. Tanner, *Ecol. Lett.* **8**, 643 (2005).
30. We thank numerous staff, students, and volunteers at the Centre for Coral Reef Biodiversity; H. Cornell; C. Schwarz; and anonymous reviewers for assistance and suggestions at various stages of the work. This research was supported by the Australian Research Council, NSF, the National Geographic Society, and James Cook University.

Global Patterns of Predator Diversity in the Open Oceans

Boris Worm,[1,2]* Marcel Sandow,[2] Andreas Oschlies,[2,3] Heike K. Lotze,[1,2] Ransom A. Myers[1]

The open oceans comprise most of the biosphere, yet patterns and trends of species diversity there are enigmatic. Here, we derive worldwide patterns of tuna and billfish diversity over the past 50 years, revealing distinct subtropical "hotspots" that appeared to hold generally for other predators and zooplankton. Diversity was positively correlated with thermal fronts and dissolved oxygen and a nonlinear function of temperature (~25°C optimum). Diversity declined between 10 and 50% in all oceans, a trend that coincided with increased fishing pressure, superimposed on strong El Niño–Southern Oscillation–driven variability across the Pacific. We conclude that predator diversity shows a predictable yet eroding pattern signaling ecosystem-wide changes linked to climate and fishing.

Humans have exploited oceanic predators such as tuna, billfish, sharks, and sea turtles for millennia. Although our knowledge of individual species has rapidly advanced, for example, through sophisticated tagging studies (1, 2), community-wide patterns of abundance and diversity are only beginning to be understood (3). This knowledge is timely. Many species have declined, are vulnerable to overfishing, or are threatened by extinction (4, 5), and there is a concern that widespread predator declines can trigger unforeseen ecosystem effects (6–8).

Effective management and conservation in the open oceans will depend on resolving the spatial distribution of multiple species, ecological communities, and fishing effort (1, 2, 9–11). Recent studies performed on a regional scale have indicated that predator species may aggregate at distinct diversity hotspots—areas of high species diversity that may represent important oceanic habitats and hold particular value for biodiversity conservation (3, 11). Yet, global-scale patterns and trends of predator diversity have remained obscure. We investigated the global distribution of predator diversity, how it relates to regional oceanography, and whether diversity has changed over time.

As a first step, we used global 5° by 5° Japanese longlining data from 1990 to 1999 to analyze contemporary patterns of tuna and bill-

[1]Biology Department, Dalhousie University, Halifax, NS, Canada B3H 4J1. [2]Leibniz Institute for Marine Science, Düsternbrooker Weg 20, 24105 Kiel, Germany. [3]National Oceanography Centre, Southampton, SO14 3ZH, UK.

*To whom correspondence should be addressed. Email: bworm@dal.ca

fish diversity (*12*). Tuna and billfish are among the most ubiquitous, ecologically important, and economically important oceanic predators, and they range globally from the equator to temperate regions (0 to ~55° latitude). Pelagic longlines are the most widespread fishing gear in the open ocean and are primarily used to target tuna and billfish. These are baited lines of up to 100 km in length that catch a wide range of predators in a similar way, operating across global scales. The Japanese logbook data represents the world's largest longline fleet and the only globally consistent data source, reporting species composition, catch, and effort for all tuna (Thunnini), billfishes (Istiophoridae), and swordfish (Xiphiidae) (table S1). We used statistical rarefaction techniques to standardize for differences in fishing effort among 5° by 5° cells and to estimate two common measures of species diversity: species richness (the expected number of species standardized per *n* individuals) and species density (the expected number of species standardized per *k* hooks) in each cell (*12, 13*). We report results that correspond to the average number of individuals (*n* = 50) and hooks (*k* = 1000) in a single longlining set. Alternative parameters (*n* = 20, 100, and 500; *k* = 500, 2000, and 5000) gave similar results. The difference between these two diversity indices is that species richness reflects solely the number of species, whereas species density reflects the number of species per unit area (*13*). Whereas richness may be more interesting ecologically, species density is more meaningful for conservation and management.

Tuna and billfish species richness (Fig. 1A) and species density (Fig. 1B) showed a consistent global pattern, indicating peaks of diversity at intermediate latitudes (15 to 30°N or S) and lower diversity toward the poles and at the equator. In the Atlantic and Indian Ocean, diversity also appeared to be higher in western regions as compared with eastern regions. Hotspots of species richness and density were clustered mostly in the subtropics, namely off the U.S. and Australian east coasts, south of the Hawaiian Islands chain, east of Sri Lanka, and most prominently in the southeastern Pacific (Fig. 1C).

We checked the generality of these results using independent scientific observer data from longline fisheries in the Atlantic and Pacific Ocean (Fig. 1, D to F). Observer records were collected by U.S. and Australian management agencies from 1990 to 1999 (*12*). They have much better taxonomic breadth (*N* = 145 species, including tuna, billfish, other bony fishes, sharks, pelagic rays, whales, dolphins, turtles, and large seabirds) but much smaller geographic range (<10%) and sample sizes (<1%) compared with the global Japanese data (table S1). Total predator richness, as calculated from the observer data, was highly correlated with the Japanese tuna and billfish data (Fig. 1, D to F), which suggests that tuna and billfish may be used to predict total predator diversity. In addition, we found a strong correlation between tuna and billfish richness with foraminiferan zooplankton diversity (Fig. 1G). Before this study, foraminifera were the only

oceanic species for which global diversity patterns were known (*14*). Remarkably, these single-celled organisms show the same latitudinal distribution as large predators, with distinct diversity peaks at intermediate latitudes (*14*). Similar patterns appear to hold for other zooplankton groups (*14*). This suggests that the global pattern of diversity shown here could be general across several trophic levels and different from latitudinal patterns on land, where diversity usually peaks around the equator (*15*).

Asking what oceanographic variables may explain global patterns of predator diversity, we explored the effects of remotely sensed sea surface temperatures (SST) (mean and spatial gradients), dissolved oxygen levels, eddy kinetic energy (calculated from sea surface height anomalies), chlorophyll *a* (mean and spatial gradients), and depth (mean and spatial gradients) on diversity, using spatial regression models (Table 1, Fig. 2, and fig. S1). These models accounted for spatial covariance among cells, while testing the relations between oceanographic variables and diversity (*12*). Most variables have been suggested to explain the distributions of individual predator species (*16*), but their effects on diversity had been unknown. Stepwise elimination of nonsignificant variables (eddy kinetic energy, depth, chlorophyll, all *P* > 0.1) revealed mean temperature, SST gradients, and oxygen as main factors (Table 1). Spatial covariance parameters indicated that latitudinal variation was much more pronounced than longitudinal variation (Table 1). Adjacent cells were prac-
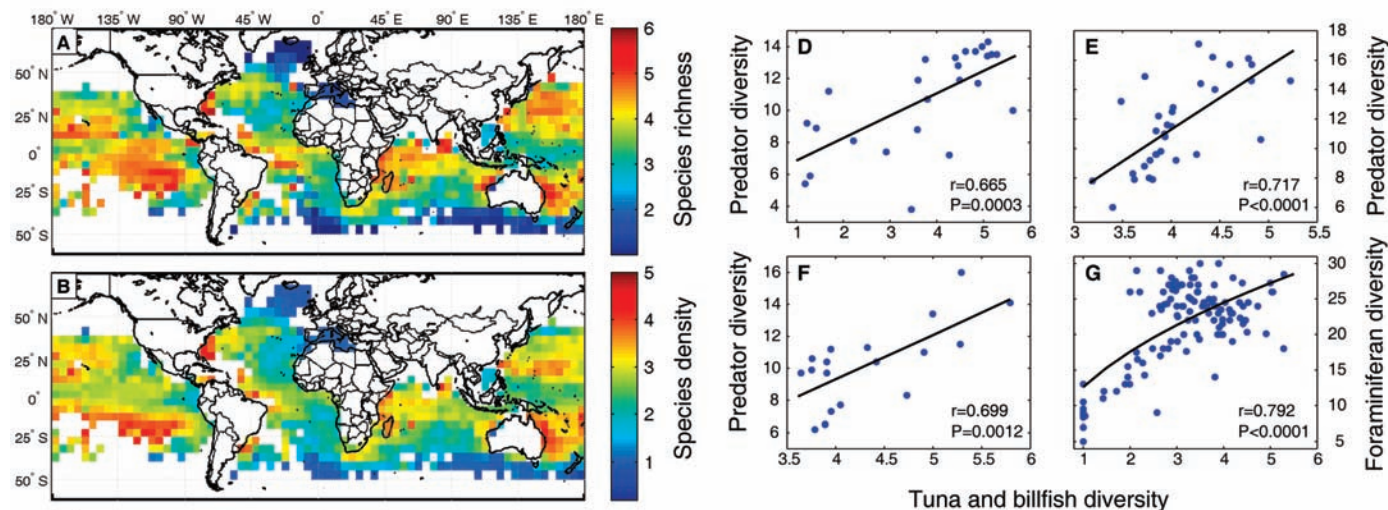
Fig. 1. Pattern and hotspots of tuna and billfish diversity. (**A**) Species richness in a standardized sample of 50 individuals. (**B**) Species density in a standardized sample of 1000 hooks. (**C**) Top 50 hotspots of species richness (yellow), species density (orange), or both (red). Hotspots represent 9% of all fished cells (6.6% of global ocean area) and correspond to the upper 25% of the range in species richness (20% for species density). (**D** to **F**) Correlations between tuna and billfish species richness and total predator richness for (D) the Northwest Atlantic (0°N to 50°N, 30°W to 100°W), (E) Hawaii (0°N to 40°N, 125°W to 180°W), and (F) Australia (10°S to 45°S, 110°E to 165°E). (**G**) Correlations between tuna and billfish species richness and foraminiferan zooplankton richness in the Atlantic Ocean (65°N to 50°S, 90°W to 20°E). Data points correspond to individual 5° by 5° cells, regression lines to best linear fits [(D) to (F)] or log-linear fits (G).

tically uncorrelated across latitude but were spatially correlated across 10° to 15° longitudinal bands.

SST (Fig. 2A) clearly emerged as the strongest predictor of species richness and species density (Table 1), showing a positive correlation over most of the observed range (5°C to 25°C) but a negative trend above 27°C mean SST (Fig. 2, D and E). For example, species richness was depressed around cool upwelling regions in the eastern Atlantic and Pacific, but also in the western tropical Pacific "warm pool" (Fig. 1A), which shows exceptionally high temperatures (>30°C) (Fig. 2A). A third-order polynomial model of SST produced the best fit for global predator diversity (Table 1 and Fig. 2, D and E). A very similar model of SST explained spatial variation in foraminiferan zooplankton diversity (14). For foraminifera, the decline of diversity at high temperatures was linked to

reduced niche availability due to a sharp, shallow thermocline in the tropical ocean (14). For tuna, which generate large amounts of metabolic heat, physiological mechanisms such as overheating at high ambient temperatures could play an additional role.

Much of the observed variation in species richness and density around the general SST trend was well explained by synoptic spatial temperature gradients (Fig. 2, B, D, and E). Sharp temperature gradients (indicated by yellow and red, Fig. 2, B, D, and E) indicate frontal zones and warm- or cold-core eddies that are associated with mesoscale oceanographic variability. Fronts and eddies often attract large numbers of species such as seabirds (17), tuna (16), turtles (2), billfish, and whales (18), likely because they concentrate food supply, enhance local production, and increase habitat heterogeneity (10, 19). Persistent fronts

also form important landmarks along transoceanic migration routes (20). Our analysis implies that these regional habitat features may also be important for global diversity.

Oxygen concentrations were positively correlated with diversity (Fig. 2C and Table 1). This is likely to relate to species physiology, because low oxygen levels (<2 ml l^{-1}) may limit the cardiac function and depth range of many tuna species (16). Regions of low oxygen are located west of Central America, Peru, and West Africa and in the Arabian Sea (Fig. 2C). Indeed, despite optimal SST around 25°C, most of these areas showed conspicuously low diversity (Fig. 1, A and B).

We analyzed temporal trends of tuna and billfish diversity since 1952, when industrial exploitation of the open oceans first expanded globally. Using recently derived correction factors for each species (21), we standardized
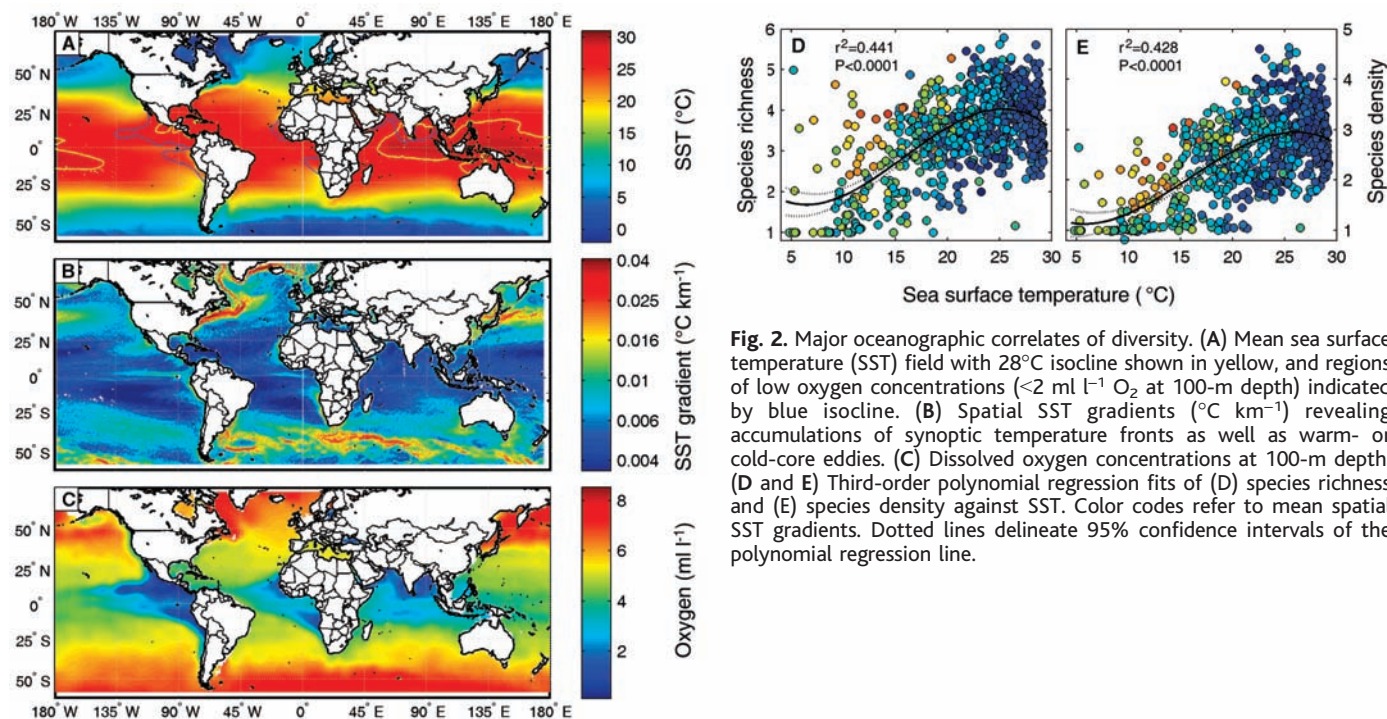
Fig. 2. Major oceanographic correlates of diversity. (**A**) Mean sea surface temperature (SST) field with 28°C isocline shown in yellow, and regions of low oxygen concentrations (<2 ml l^{-1} O$_2$ at 100-m depth) indicated by blue isocline. (**B**) Spatial SST gradients (°C km^{-1}) revealing accumulations of synoptic temperature fronts as well as warm- or cold-core eddies. (**C**) Dissolved oxygen concentrations at 100-m depth. (**D** and **E**) Third-order polynomial regression fits of (D) species richness and (E) species density against SST. Color codes refer to mean spatial SST gradients. Dotted lines delineate 95% confidence intervals of the polynomial regression line.

Table 1. Spatial regression model relating tuna and billfish diversity to oceanography. Regression coefficients and their standard error estimates (SE) are given, along with test statistics. Covariance parameters estimate spatial correlation among 5° by 5° cells, assuming an anisotropic exponential decay model: $cov(y_i, y_j) = \sigma^2 \exp - (\theta_1 d_{i,j,1} + \theta_2 d_{i,j,2})$, where θ_1 describes the latitudinal and θ_2 the longitudinal covariance parameter, $d_{i,j,1}$ the latitudinal distance, and $d_{i,j,2}$ the longitudinal distance between cells y_i and y_j.

Variable	Species richness		t	P	Species density		t	P
	Coefficient	SE			Coefficient	SE		
Intercept	1.694	0.846	2.0	0.1833	0.887	0.630	1.4	0.2945
Sea surface temperature	−0.443	0.153	−2.9	0.0038	−0.342	0.115	−3.0	0.0030
(SST)^2	0.04	0.009	4.3	<0.0001	0.030	0.007	4.3	<0.0001
(SST)^3	−0.001	0.0002	−4.5	<0.0001	−0.001	0.0002	−4.4	<0.0001
SST gradient	48.69	13.7	2.9	0.0042	29.617	9.830	3.0	0.0027
Dissolved oxygen	0.166	0.0495	3.4	0.0008	0.173	0.039	4.5	<0.0001
Covariance parameters	θ_1	θ_2	σ^2		θ_1	θ_2	σ^2	
Estimates	0.242	0.089	0.475		0.179	0.071	0.267	
Likelihood ratio test	df = 2	X^2 = 64.4	P < 0.0001		df = 2	X^2 = 139.7	P < 0.0001	

Japanese longline data for historical changes in fishing practices, specifically the increase in longline depth during the 1970s and 1980s to target deeper swimming species such as bigeye tuna (*Thunnus obesus*). Species richness and species density were calculated from these data by rarefaction, as outlined above. Resulting data sets are displayed in Movies S1 and S2. To extract seasonal, interannual, and decadal trends, we estimated changes in average species richness and species density across the Atlantic (Fig. 3A), Indian (Fig. 3B), and Pacific Oceans (Fig. 3C), using linear mixed effects models that accounted for spatial autocorrelation and for changes in the spatial and seasonal coverage of fished cells (*12*).

Results indicated that interannual variation was an order of magnitude stronger than seasonal variation (table S2). Species richness showed pronounced year-to-year fluctuations and decadal declines of 10% to 20% in all oceans (Fig. 3, A and C). However, this pattern reversed in the Pacific in 1977, when richness began to increase again to pre-exploitation levels (Fig. 3C). Species density showed gradual ~50% declines in the Atlantic (Fig. 3A) and Indian Oceans (Fig. 3B) and ~25% decline in the Pacific (Fig. 3C). These declines were most pronounced in intensely fished tropical areas, particularly in the Indian and Atlantic Oceans (Movies S1 and S2). The trajectories of species richness and, particularly, species density were negatively correlated with 5- to 10-fold increases in total catch of tuna and billfish in all oceans since 1950 (Fig. 3, A to C), which may have led to regional depletion of vulnerable species (*4*, *5*, *22*). Larger declines in species density likely result from the combined effects

of decreasing richness and decreasing abundance over time. Although strong temporal autocorrelation in these trends precluded statistical inference, we could not identify a factor other than fishing that may plausibly explain long-term, global-scale declines. Gradual ocean warming, for example, may lead to increased diversity over most of the observed range (Fig. 2, D and E, and results below), although the effects of complex changes in current patterns and regional oceanography are hard to predict. To explore historic trends in temperature and to test the predictive value of our oceanographic model (Table 1) over time, we fitted it to depth-corrected diversity and SST data from the 1960s, 1970s, 1980s, and 1990s. We found that relations among sea surface temperature, SST gradients, oxygen, and diversity were very similar across the last four decades (table S3). These findings may suggest that there were no major decadal changes in the relations between diversity and oceanography.

Short-term variability in species richness, however, appeared to be linked to climate, at least in the Pacific. Pronounced year-to-year changes in species richness D (expressed as first difference $\Delta_t = D_{t+1} - D_t$) showed a strong positive correlation ($r = 0.54$, $P < 0.0001$) with the El Niño–Southern Oscillation (ENSO) index (Fig. 3D). When we analyzed this pattern spatially at the level of individual cells, we saw that widespread increases in species richness during El Niño warm phases occurred across the North and South Central Pacific (Fig. 3E). This could be linked to regional warming and concomitant changes in recruitment or movement of species into these areas; changes in catch-

ability could also be a factor. Substantial decreases in species richness were seen in the tropical Eastern Pacific, a region that suffers from greatly reduced productivity and associated mass mortality of marine life during El Niño (Fig. 3E). Indeed, we found that several large predator species (such as Indo-Pacific blue marlin, *Makaira mazara*) (Fig. 3F) showed lower abundance in the tropical Eastern Pacific and apparent increases across the North and South Central Pacific with increasing El Niño conditions. This is probably not an effect of changing catchability. Surface-dwelling species such as marlins would likely extend their vertical range with the deepening of the thermo- and oxyclines during El Niño events in the Eastern Pacific. Hence, they would become more catchable because they are more likely to intercept longlines, which are currently set at a mean depth of ~100 m and a maximum of 400 m (*21*). The observed pattern (Fig. 3F) is the opposite and is more consistent with ENSO-induced migration of highly mobile predators to favorable areas. This hypothesis may be tested further using satellite tracking data currently being gathered for a wide range of Pacific predators (*23*).

In the Indian Ocean, ENSO or the Indian Ocean Dipole Index (*12*) did not appear to influence species richness or density ($P > 0.2$). In the Atlantic, however, we detected a weak positive trend of species richness with the North Atlantic Oscillation Index (NAO) ($r = 0.301$, $P = 0.062$) and, in the Pacific, a significant correlation of species richness with the Pacific Decadal Oscillation Index (PDO) ($r = 0.306$, $P = 0.035$), which may be linked to long-term changes in the ENSO regime (*24*).
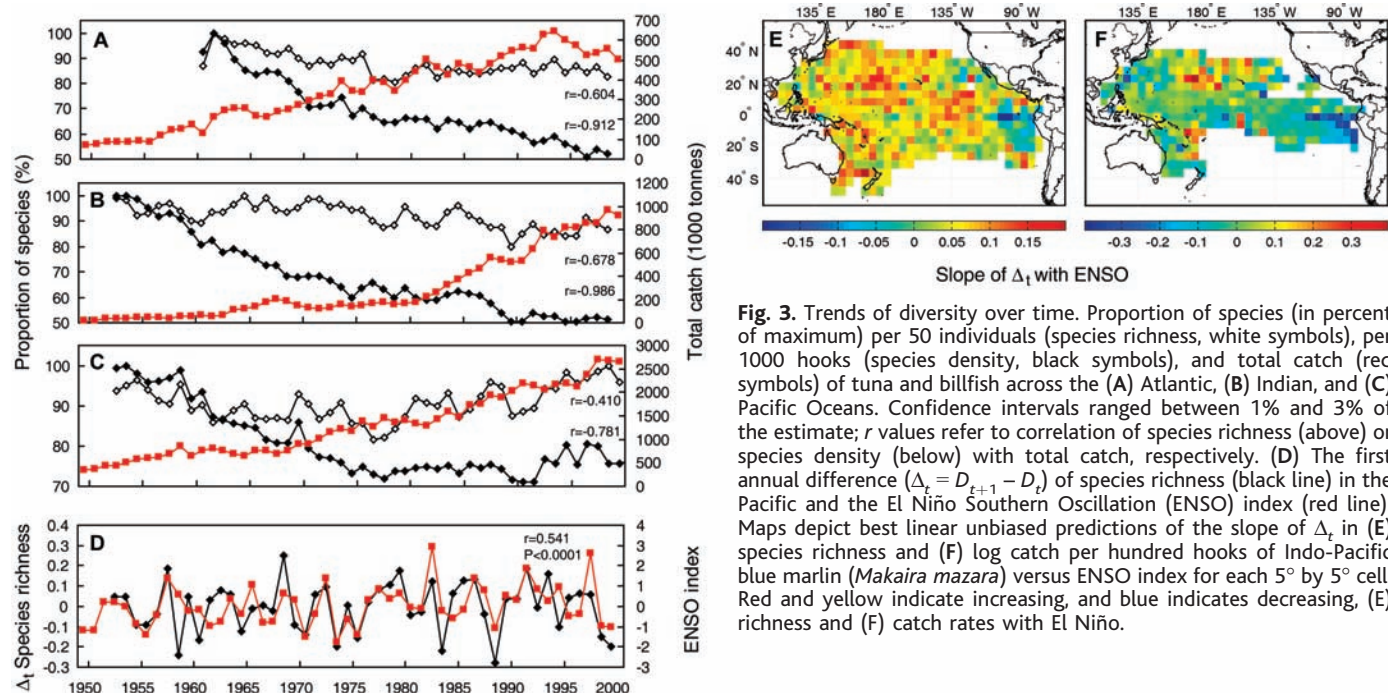
Fig. 3. Trends of diversity over time. Proportion of species (in percent of maximum) per 50 individuals (species richness, white symbols), per 1000 hooks (species density, black symbols), and total catch (red symbols) of tuna and billfish across the (**A**) Atlantic, (**B**) Indian, and (**C**) Pacific Oceans. Confidence intervals ranged between 1% and 3% of the estimate; r values refer to correlation of species richness (above) or species density (below) with total catch, respectively. (**D**) The first annual difference ($\Delta_t = D_{t+1} - D_t$) of species richness (black line) in the Pacific and the El Niño Southern Oscillation (ENSO) index (red line). Maps depict best linear unbiased predictions of the slope of Δ_t in (**E**) species richness and (**F**) log catch per hundred hooks of Indo-Pacific blue marlin (*Makaira mazara*) versus ENSO index for each 5° by 5° cell. Red and yellow indicate increasing, and blue indicates decreasing, (**E**) richness and (**F**) catch rates with El Niño.

When the PDO suddenly reversed to a warm phase in 1977, famously inducing a basin-wide regime shift (25), the trajectory of predator species richness also reversed (Fig. 3C).

Although other studies have confirmed the effects of climate perturbations on movement and recruitment of individual species (25, 26), this is the first account of any ocean-wide changes in community diversity. We suggest that our results reconcile the different effects of fishing and climate, a matter of intense debate (27). We propose that fishing may primarily drive long-term, low-frequency variation in fish communities through gradual changes in species abundance, composition, and size (28), whereas climate induces year-to-year variation that may modify decadal trends only in cases where lasting regime shifts occur (25).

These results establish a dynamic global pattern of tuna and billfish diversity through space and time. Detailed data for other predators and zooplankton strongly suggest that at least the spatial pattern could be general across taxonomically distant species groups. However, we caution that there are likely some important exceptions. Marine mammals, for example, may show high seasonal diversity in subpolar regions, such as the Bering Sea (7). Also, the coarse resolution of our data may mask smaller scale (<100 km) variation associated, for example, with coastal habitats or seamounts (11). More work is needed to resolve such variation, particularly in nearshore regions. At the global scale examined here, sea surface temperature, SST gradients, and oxygen were consistently correlated with species diversity across at least four decades. Optimal habitats that attract numerous species appeared to be characterized mainly by warm waters (~25°C) with sufficient oxygen concentrations (>2 ml l^{-1}) in combination with mesoscale oceanographic gradients, resulting in the formation of feeding habitats around thermal fronts and eddies. Fine-scale experimental studies confirm the importance of temperature and oxygen levels, as well as food concentrations for single predator species (2, 9, 16, 29). Here, we have shown that these variables also correlate with global diversity patterns, despite large regional differences in environmental conditions and species identities.

These results can be used to inform conservation and management of the high seas. First, species richness and density as calculated from standardized longlining data appear to be sensitive indicators of community-wide changes that may integrate the effects of both fishing and climate as major agents of change. Second, knowledge of global diversity patterns, when merged with fine-scale information on habitat use, spawning areas, migration patterns, and fishing mortality (1, 2, 9), could be used to define priority areas for ocean conservation. Current conservation efforts such as the international High-Seas Marine Protected Area Initiative (30) may thereby direct limited resources efficiently and maximize conservation benefits for the future. These efforts appear even more urgent when considering ocean-scale declining trends in predator diversity as seen in our data. We caution that these trends are based on common target species. Incorporating information on vulnerable bycatch species such as sharks (22) and sea turtles (2) might prove these estimates conservative.

References and Notes
1. B. A. Block et al., Science 293, 1310 (2001).
2. S. Ferraroli, J.-Y. Georges, P. Gaspar, Y. L. Maho, Nature 429, 521 (2004).
3. D. Malakoff, Science 304, 1104 (2004).
4. D. Pauly et al., Nature 418, 689 (2002).
5. R. A. Myers, B. Worm, Philos. Trans. R. Soc. Lond. B Biol. Sci. 360, 13 (2005).
6. S. P. Cox et al., Can. J. Fish. Aquat. Sci. 59, 1736 (2002).
7. A. M. Springer et al., Proc. Natl. Acad. Sci. U.S.A. 100, 12223 (2003).
8. N. K. Dulvy, R. P. Freckleton, N. V. C. Polunin, Ecol. Lett. 7, 410 (2004).
9. A. Bertrand, E. Josse, P. Bach, L. Dagorn, Can. J. Fish. Aquat. Sci. 59, 1002 (2002).
10. K. D. Hyrenbach, K. A. Forney, P. K. Dayton, Aquat. Conserv. Mar. Freshw. Ecosyst. 10, 43 (2000).
11. B. Worm, H. K. Lotze, R. A. Myers, Proc. Natl. Acad. Sci. U.S.A. 100, 9884 (2003).
12. Detailed methods are available as supporting material on Science Online.
13. N. J. Gotelli, G. R. Graves, Null Models in Ecology (Smithsonian Institution Press, Washington DC, 1996).
14. S. Rutherford, S. D'Hondt, W. Prell, Nature 400, 749 (1999).
15. H. Hillebrand, Am. Nat. 163, 192 (2004).
16. P. N. Sund, M. Blackburn, F. Williams, Oceanogr. Mar. Biol. Annu. Rev. 19, 443 (1981).
17. J. C. Haney, Mar. Ecol. Prog. Ser. 28, 279 (1986).
18. P. Etnoyer, D. Canny, B. Mate, L. Morgan, Oceanography 17, 90 (2004).
19. A. Oschlies, V. Garçon, Nature 394, 266 (1998).
20. J. J. Polovina, E. Howell, D. R. Kobayashi, M. P. Seki, Prog. Oceanogr. 49, 469 (2001).
21. P. Ward, R. A. Myers, Can. J. Fish. Aquat. Sci. 62, 1130 (2005).
22. J. K. Baum et al., Science 299, 389 (2003).
23. B. A. Block, D. P. Costa, G. W. Boehlert, R. E. Kochevar, Oceanol. Acta 25, 255 (2003).
24. M. Newman, G. P. Compo, M. A. Alexander, J. Clim. 16, 3853 (2003).
25. N. J. Mantua, S. R. Hare, Y. Zhang, J. M. Wallace, R. C. Francis, Bull. Am. Meteorol. Soc. 78, 1069 (1997).
26. P. Lehodey, F. Chai, J. Hampton, Fish. Oceanogr. 12, 483 (2003).
27. B. Worm, R. A. Myers, Nature 429, 15 (2004).
28. P. Ward, R. A. Myers, Ecology 86, 835 (2005).
29. J. M. Blank, J. M. Morrissette, P. S. Davie, B. A. Block, J. Exp. Biol. 205, 1881 (2002).
30. IUCN, Ten-Year High Seas Marine Protected Area Strategy (International Union for Conservation of Nature and Natural Resources, Gland, Switzerland, 2004).
31. We gratefully acknowledge access to longline fishing data by the Japanese Fishery Agency, NOAA National Marine Fisheries Service, and the Australian Fishery Management Agency. We thank S. Rutherford, S. D'Hondt, and W. Prell for the foraminiferan data and R. Watson, the Sea Around Us Project, and the UN Food and Agriculture Organization for providing global catch data. Oceanographic data were provided by the Goddard Earth Sciences Data Services Center, the Physical Oceanography Distributed Active Archive Center, the CLS Space Oceanography Division, the NOAA Cooperative Institute for Research in Environmental Sciences climate diagnostic center, and the Climate Research Unit at the University of East Anglia. We thank W. Blanchard for statistical advice and technical support, and J. Baum, K. Gjerde, K. Kaschner, N. Mantua, A. Ottensmeyer, D. Pauly, C. Peterson, W. Prell, and P. Ward for comments. We acknowledge funding by The Sloan Foundation (Census of Marine Life, Future of Marine Animal Populations program), Deutsche Forschungsgemeinschaft, The Pew Charitable Trusts, and the Natural Sciences and Engineering Research Council of Canada.

Nuclear Reprogramming of Somatic Cells After Fusion with Human Embryonic Stem Cells

Chad A. Cowan, Jocelyn Atienza, Douglas A. Melton, Kevin Eggan*

We have explored the use of embryonic stem cells as an alternative to oocytes for reprogramming human somatic nuclei. Human embryonic stem (hES) cells were fused with human fibroblasts, resulting in hybrid cells that maintain a stable tetraploid DNA content and have morphology, growth rate, and antigen expression patterns characteristic of hES cells. Differentiation of hybrid cells in vitro and in vivo yielded cell types from each embryonic germ layer. Analysis of genome-wide transcriptional activity, reporter gene activation, allele-specific gene expression, and DNA methylation showed that the somatic genome was reprogrammed to an embryonic state. These results establish that hES cells can reprogram the transcriptional state of somatic nuclei and provide a system for investigating the underlying mechanisms.

The generation of embryonic stem (ES) cell lines and cloned animals by somatic cell nuclear transfer has demonstrated that the cytoplasm of an oocyte can reprogram the genome of a somatic cell to an embryonic state (1, 2). There is considerable interest in how reprogramming